Automated cardiac event change detection for continuous remote patient monitoring devices

Conference Paper · December 2011

DOI: 10.1145/2185216.2185281

3 authors:

Britty Baby
Indian Institute of Technology Delhi
28 PUBLICATIONS **206** CITATIONS
SEE PROFILE

M. Sabarimalai Manikandan
Indian Institute of Technology Bhubaneswar
77 PUBLICATIONS **1,807** CITATIONS
SEE PROFILE

Soman Kp
Amrita Vishwa Vidyapeetham
769 PUBLICATIONS **9,859** CITATIONS
SEE PROFILE

Automated Cardiac Event Change Detection for Continuous Remote Patient Monitoring Devices

Britty Baby
Department of Electronics and Communication Engineering, Amrita Vishwa Vidyapeetham, Tamilnadu, India-641112.

M. Sabarimalai Manikandan
Center for Excellence in Computational Engineering and Networking Amrita Vishwa Vidyapeetham, Tamilnadu, India-641112.
msm.sabari@gmail.com

K. P. Soman
Center for Excellence in Computational Engineering and Networking Amrita Vishwa Vidyapeetham, Tamilnadu, India-641112.

ABSTRACT

Recently, wireless body area network (WBAN) plays an important role in remote cardiac patient monitoring, and mobile healthcare applications. Generally, the use of WBAN technology is restricted by size, power consumption, transmission capacity (bandwidth), and computational loads. In this paper, we therefore propose an automated cardiac event change detection for continuous remote patient monitoring devices. The proposed event change detection algorithm consists of two stages: i) ECG beat extraction; and ii) ECG beat similarity measure. In the first stage, the onset of each QRS complex is identified using the Gaussian derivative based QRS detector and the two heuristics rules. In the second stage, we employ the weighted wavelet distance (WWD) metric for finding the similarity between two ECG beats in wavelet domain. The WWD is the weighted normalized Euclidean wavelet distance between the wavelet subband coefficients vectors of the current and past ECG beats, where weights are equal to the relative wavelet subband energies of the corresponding subbands. The experimental results show that the weighted wavelet distance measure works substantially better than the conventional PRD and the wavelet based weighted PRD (WWPRD) measures under noisy environments. The proposed approach has been tested and yielded an accuracy of 99.76% on MIT-BIH Arrhythmia Database.

Keywords

electrocardiogram, QRS detection, cardiac event detection, peak-finding logic, Gaussian derivative, remote cardiac patient monitoring, wavelet distance metric.

1. INTRODUCTION

In recent years, wireless remote health monitoring system is widely used for screening, diagnosis and management of cardiac diseases of post-surgical patients and chronic heart failure patients. Cardiac patients with wireless wearable and/or implant medical devices can be checked remotely no matter where they are located. Cardiologists can monitor and access cardiac data of any patient by connecting the mobile devices such as mobile phones, smartphones, personal digital assistants (PDAs), and wireless-enabled (Wi-Fi) laptops to telemedicine network using any of wireless and cellular technologies such as Wi-Fi, Bluetooth, GSM, GPRS, CDMA, WiMAX, UMTS, CDPD, Mobitex, 4G, and satellite-internet technology. The remote patient monitoring system has the following advantages: i) monitoring and accessing subjects who are mobile and may reduce hospital readmissions; ii) time-saving and cost-effective means for follow-up; iii) continuous monitoring decreases the risk factors of life threatening cardiac diseases; iv) supports emergency patient promptly and appropriately; v) provides the better privacy and peace of mind for patients and extensive care from family members. The electrocardiogram (ECG) records the electrical activity of the heart that can be useful to detect signs of poor blood flow, heart muscle damage, abnormal heartbeats, and other heart problems. The continuous recording and monitoring of ECG signal can play a major role in prevention of cardiovascular disease. For clinical evaluation of hospitalized cardiac patients, the ECG signal is recoded for duration of 12-48 hours using an ECG Holter device. Then, the clinical evaluation of long-term ECG signal is performed by physicians. The recent advancements in microelectronics, digital signal processing techniques and wireless communication technologies enable cardiologists to provide medical treatment by monitoring remotely located ambulatory, post-surgical, and chronic cardiac patients. Although the wearable cardiac monitoring device collect and transmit the vital signs of cardiac patients continuously, there are limitations in the use of wireless sensor network technology and wearable devices. Generally, the use of wireless wearable cardiac monitoring device is restricted by size, power consumption, transmission capacity (or bandwidth), memory, and computational loads. Recent growth in 2G and 3G technologies enable to access remote patient cardiac information by cardiologists at any time and location. Although, these technologies provide high bandwidth, public highly demands cost-effective healthcare services. Moreover, the continuous cardiac monitoring device reduces more power for transmission and thus reduces the battery life.

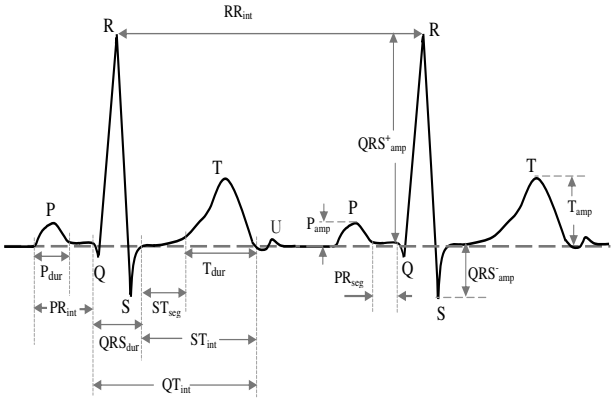

Figure 1: The electrocardiogram (ECG) signal and some diagnostic parameters.

In such scenarios, there is a great demand for an automated cardiac event change detector for continuous patient monitoring applications. The limitations of continuous wireless patient monitoring system can be overcome by exploiting and exploring the patterns of ECG beat in the long-term ECG signal. In this work, we propose an automated cardiac change detection algorithm for pervasive and continuous wireless cardiac monitoring devices. The proposed cardiac monitoring system not only reduces the transmission and storage cost and power consumption, but also alerts the cardiologists and instantly sends only beat patterns which exhibit abrupt changes in the ECG signal. In literature, many algorithms have been developed for classification of ECG beats and detection of ST pattern change. The ECG beat classification algorithms are based on wavelet features, ECG morphology and RR interval features, neural networks, higher order statistics, hermite basis function, support vector machines, fuzzy logic, and principal component analysis. It is well-known that the analytic features capture local information in a ECG signal. But the extraction of the analytic features is very difficult and challenging task under noise environments. Moreover, performance of any ECG beat recognition system highly relies on the accuracy of the QRS complex detector. The beat classification approach based on the ECG templates and distance measure is heavily affected by various kinds of noise.

This paper is organized as follows. Section 2 describes the characteristics of ECG beats in a long-term ECG signal. Section 3 presents cardiac event change detection algorithm based on the ECG beat extractor and weighted wavelet distance metric. The experimental results of the proposed approach for the well-know MIT-BIH arrhythmia database are presented in Section 4. Finally, conclusions are drawn in the Section 5.

2. PRELIMINARIES

The electrocardiogram (ECG) continues to be a critical component of the evaluation of patients who have signs and symptoms of emergency cardiac conditions [1]. Cardiac impulses normally originate in the sinoatrial (SA) node and then are conducted through the atrial tissue to the atrioventricular (AV) node and into the bundle of His [2]. The

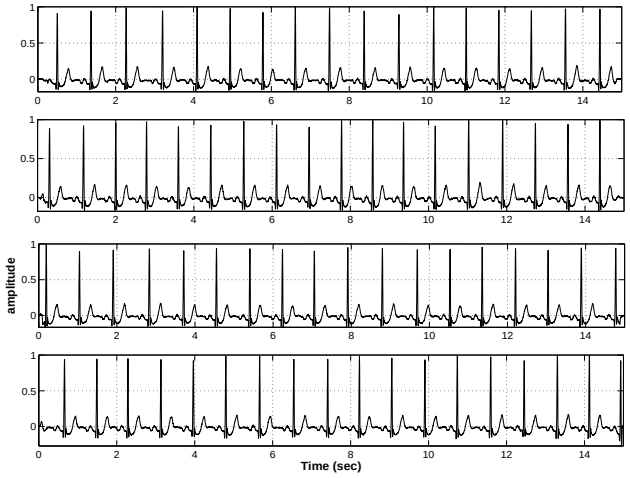

Figure 2: One-minute ECG signal taken from 103 illustrates the similarity between successive ECG beats.

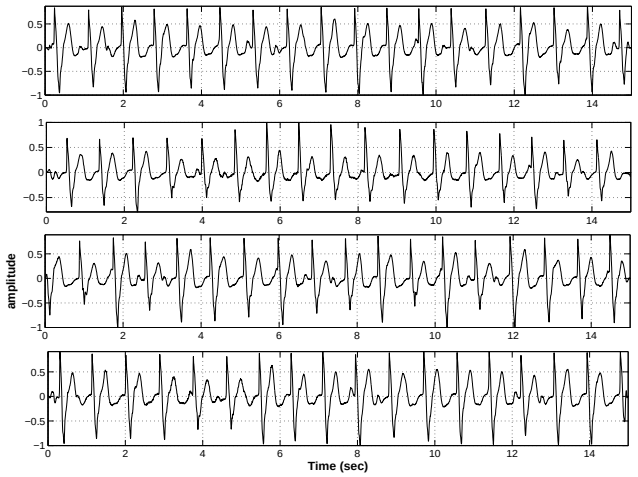

Figure 3: One-minute ECG signal taken from record 107 illustrates the dissimilarity between successive ECG beats.

ECG signal represents the changes in electrical potential in the cardiac muscles during the cardiac cycle as recorded on the surface of the body. A two cycle ECG signal with various amplitudes and time intervals is shown in Fig. 1. Any change in the cardiac rhythm or activity is clearly visible in the PQRST morphologies. The complete PQRST morphology is referred to as ECG beat or cycle. Generally, a normal ECG signal consists of local waves such as P wave, QRS complex, and T wave. Computer aided cardiac diagnosis extracts durations (P wave, QRS complex, T wave), intervals (PR interval, QT interval, RR interval), segments (PR segment, ST segment), amplitudes, shapes of local waves of ECG signal and also heart rate. In most of the normal cases, the inter ECG beat patterns are similar in long-term ECG recordings. Even in the arrhythmia cases, the inter ECG patterns are similar for a short duration. The significance of similar ECG patterns may not play a major role in diagnosis of heart problems and only change in the ECG patterns pro-

vide accurate clinical information of the cardiac abnormality at particular time instants. The one-minute ECG signals from the records 103 and 107 are shown in Figs. 2 and 3. Each plot in Fig. 2 is the 15-second duration ECG signal. We can notice that the variation across the ECG beats is negligible in the case of ECG signal from the record 103 as shown in Fig. 2. Meanwhile, the ECG signals in Fig. 2 show that there is a beat pattern change after 15 second which is shown in second plot of Fig. 3. It shows that the limitations of wireless wearable medical devices that are mentioned in the Introduction Section are rectified with noise robust event change detection algorithm.

The amplitude of the ECG signal as measured on the skin ranges from 0.1 mV to 5 mV [9]. The recommendations of the committee on electrocardiography of the American heart association suggest a conversion rate of 500 HZ with a 9-bit precision [3]. In practice, sample rates from 100 Hz to 1000 Hz are used with 8-bit to 16-bit precision [9]. The information rate is thus approximately 11-22 Mbits/hour/lead. The basis of standard clinical electrocardiography is the 10-second 12-lead ECG [4]-[6]. During each particular phase of clinical testing, 10-second 12-lead ECGs are recorded from the subjects in the study and these are then analyzed to determine any cardiac abnormalities [4]. The usual duration of computer evaluated ECG records is 10-second, which typically contain a number of heartbeats and hence a number of diagnostic parameters such as amplitude, duration, interval, and shape of the ECG beat. In this work, we therefore process an ECG segment with duration of 10-second.

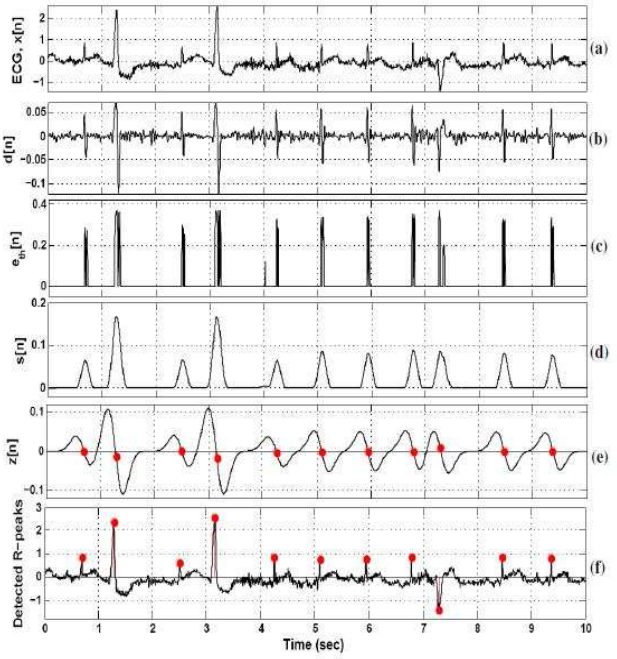

Figure 5: (a) ECG signal, (b) Differenced filtered signal, (c) Thresholded energy signal $\tilde{e}_{th}[n]$, (d) Shannon energy (SE) envelope, (e) Convolved output of the SE envelope with FOGD operator and (f) Detected R peaks.

3. CARDIAC EVENT CHANGE DETECTION ALGORITHM

3.1 ECG Beat Extraction

In this work, QRS complexes are detected using an algorithm reported in our previous work [15]. This algorithm uses Shannon energy transformation to obtain the QRS complex envelope of the filtered ECG signal and the first-order Gaussian differentiator for determining location of candidate R-peaks in the envelope. The simplified block diagram of the QRS detection algorithm is shown in Fig. 4(a), which consists of the following steps: i) QRS complex enhancement; ii) squaring and thresholding; iii) Shannon energy and smoothing; iv) first-order Gaussian differentiator (FOGD)-based peak finding task; and v) finding time instant of true R-peak. The original ECG signal and the forward difference of the filtered signal (dECG) are shown in Fig. 5(a) and (b). The output of thresholding step is shown in Fig. 5(c). This smoothing process generates peaks corresponding to the QRS-complex portions and its output is depicted in Fig. 5(d). The 1080-point Gaussian window with spread $\sigma = 45$ is shown in Fig. 4(b) and the corresponding FOGD is shown in Fig. 4(c). Due to the anti-symmetric nature of the FOGD, the convolved output $z[n]$ shown in Fig. 5(e) has zero-crossings around the peaks of the envelope $s[n]$. Hence, the zero-crossings accompanied by positive to negative transition are detected and used as guides to find locations of real R peaks in the signal. A simple rule identifies the real R-peak in the ECG within ± 25 samples of the detected peak in the envelope $s[n]$. Fig. 5(f) clearly shows that the R peaks can be accurately detected regardless of varying amplitudes and shapes of QRS complexes and noise.

3.2 The Weighted Wavelet Distance Measure

The wavelet transform (WT) provides a description of the signal in the time-scale domain, allowing the representation of the temporal features of a signal at different resolutions. Therefore, it is a suitable tool to analyze the ECG signal which is characterized by local wave patterns (QRS complexes, P and T waves) with different frequency content. Moreover, the noise and artifacts appear at different frequency bands, thus having different contribution at various scales [10]. The information can be organized in a hierarchical scheme of nested subspaces called multiresolution analysis in $L^2(\Re)$. In multiresolution signal decomposition (MSD), the signal $x(t) \in L^2(\Re)$ is decomposed to detailed and approximated versions using the scaled and translated versions of the wavelet ($\psi_{j,k}(t)$) and scaling functions ($\phi_{j,k}(t)$). The approximations are the low-frequency components of the signal and the details are the high-frequency components. The MSD is used to exploit two important issues. The first is the localization property in time and will appear by the presence of large coefficients at the time. The second property is the partitioning of the signal energy at different frequency bands. The MSD for a given signal $x(t)$ is given by

$$x(t) = \sum_{k=-\infty}^{\infty} \mathrm{A}_J(k)\phi_{J,k}(t) + \sum_{j=1}^{J}\sum_{k=-\infty}^{\infty} \mathrm{D}_j(k)\psi_{j,k}(t) \qquad (1)$$

with $\mathrm{A}_J(k) = \int_{-\infty}^{\infty} x(t)\phi_{J,k}(t)dt$ and $\mathrm{D}_j(k) = \int_{-\infty}^{\infty} x(t)\psi_{j,k}(t)dt$ where J is the number of decomposition levels, $\mathrm{A}_J = \{\mathrm{a}_J(k)\}_{k\in Z}$ are the approximation coefficient vectors at resolution level J and

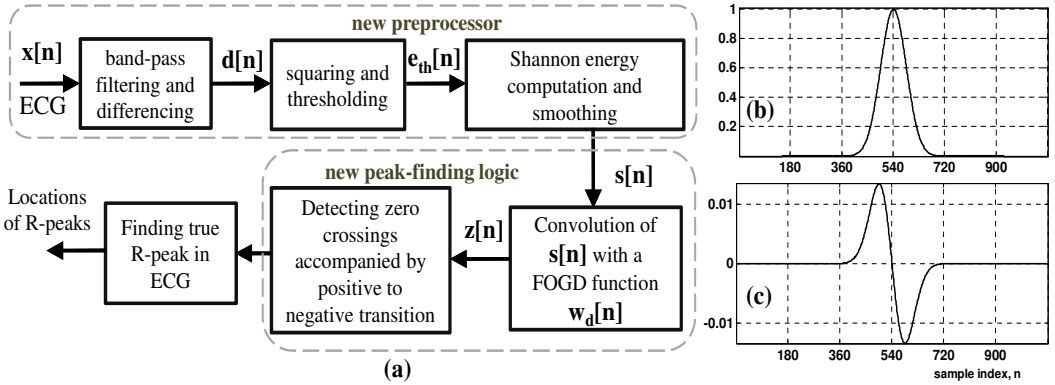

Figure 4: (a) Block diagram of the proposed R-peak detector, (b) 1080-point Gaussian window with spread $\sigma = 45$ and (c) First-order Gaussian differentiator (FOGD).

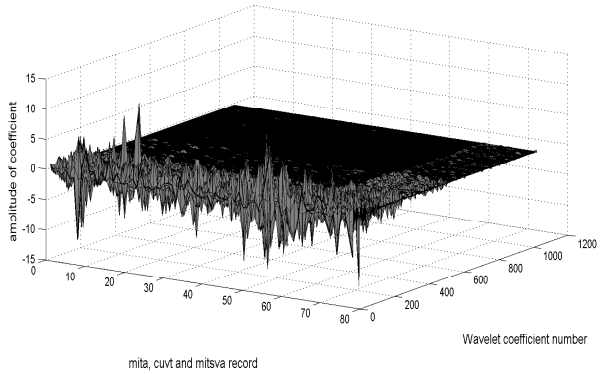

Figure 6: Subband coefficients obtained by five-level decomposition of the ECG signal blocks taken from from `mita`, `cuvt` and `mitsva` databases using a BW 9/7-tap wavelet filter set. Black indicates the least active regions and gray depicts the most active regions. Large coefficients toward low frequency subbands and, more importantly, spatial clustering of the wavelet coefficients within each subband.

$\{\mathrm{D}_j = \{\mathrm{d}_j(k)\}_{k\in Z}\}_{j=1,2,\ldots J}$ are the detail coefficient vectors. The wavelet coefficients vector is given by $\mathrm{C} = [\mathrm{D}_1\ \mathrm{D}_2\ \mathrm{D}_3 \cdot \cdot \cdot \mathrm{D}_J\ \mathrm{A}_J]$. The signal $x(n)$ can be expressed as the summation of approximation $\mathrm{A}_J(n)$ signals and detail $\{\mathrm{D}_j(n)\}_{1\le j\le J}$ signals, that is:

$$x(n) = \sum_{j=1}^{J} \mathrm{D}_j(n) + \mathrm{A}_J(n), n = 1,\ 2,\ 3.....N. \qquad (2)$$

For example, if a five-level decomposition of the signal is done, it results in one approximation signal (low-frequency) and five detail signals (high- and intermediate-frequency).

In practice, the amplitude distributions of the wavelet coefficients of subbands are different due to varying characteristics of ECG morphologies. Therefore, an analysis of amplitude distribution of the wavelet coefficients is essential for an effective data compression and will be discussed in this section. Seventy-eight 1024 sample segments of ECG signals are selected from three different ECG databases, 15 each from the MIT-BIH Supraventricular arrhythmia (`mitsva`) database (128 Hz, 10 b/sample), the Creighton university ventricular tachyarrhythmia `cuvt` database (250 Hz, 12 b) and 48 from the MIT-BIH arrhythmia (`mita`) database (360 Hz, 11 b). The 78 signal blocks are decomposed up to five-level using a BW 9/7-tap wavelet filter set and their amplitude distributions of wavelet coefficients are shown in Fig. 6. Black (low active regions) and gray (high active regions) in the figure represent the smaller amplitude wavelet coefficients and larger amplitude coefficients, respectively. For all the signal blocks, high activity regions toward low frequency subbands and these regions are most important for perfect reconstruction. It shows that the WT of most ECG signals are sparse, resulting in a large number of small coefficients and a small number of large coefficients. We notice that the noise is well explained by a few levels that contain fine details and its effect disappears at the coarser scales which is shown in Fig. 6. A measure of amplitude distribution of coefficients within the subbands is important to know the degree of importance. The wavelet subband energy (WSE) gives a good measurement of information of the signal contents and can be exploited to characterize the signal and noise contents. The relative wavelet subband energies of the subbands of the decomposed ECG signals are shown in Fig. 7. We notice that the subbands D_1 and D_2 contain most of the energy attributed to the noise and that the noise energy is practically nonexistent at the lower subbands. The relative wavelet subband energy estimate provides local information associated to the different frequency subbands present in the ECG segment and their corresponding degree of importance. Thus, the wavelet energy estimates are used as weights to characterize the local clinical distortions of the compressed signal.

Let A_J be the approximation and $\mathrm{D}_J, \mathrm{D}_{J-1}, ..., \mathrm{D}_1$ be the details in a J-level WT. The amplitude distribution of the wavelet coefficients of the decomposed ECG signals are shown in Fig. 6. The total energy of the wavelet coefficients E_t is expressed as

$$E_t = E_{\mathbf{A}_J} + \sum_{j=1}^{J} E_{\mathbf{D}_j} = \sum_{k=1}^{N_{A_J}} |A_J(k)|^2 + \sum_{j=1}^{J} \sum_{k=1}^{N_{D_j}} |D_j(k)|^2 \quad (3)$$

where N_{A_J} and N_{D_j} are the lengths of the approximation

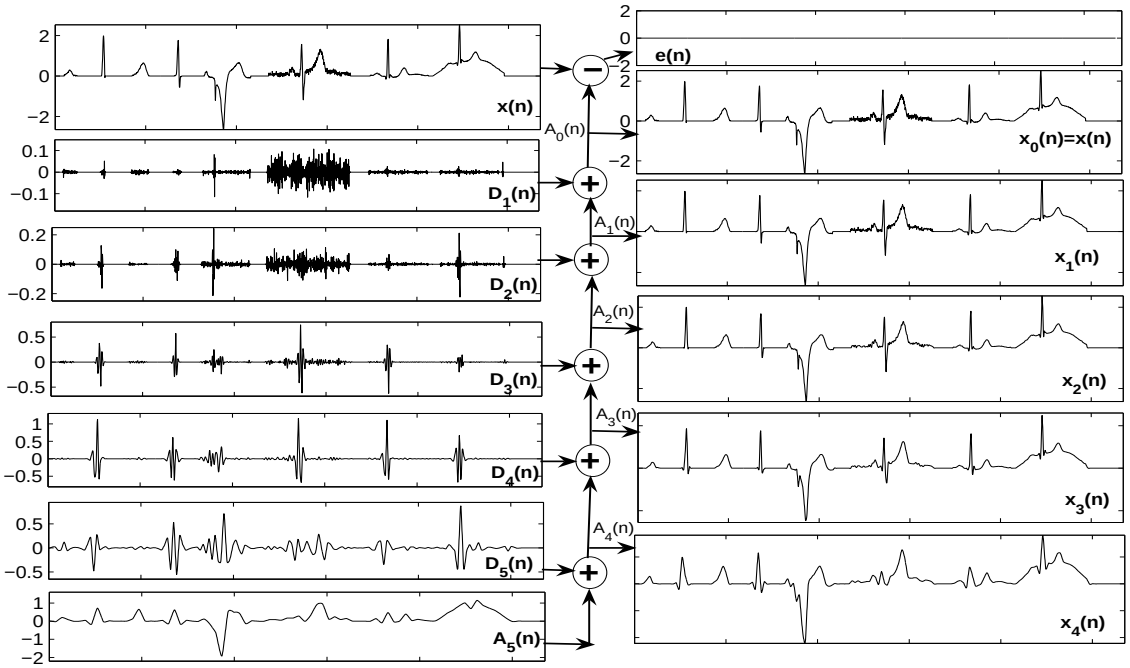

Figure 8: The synthesis (reconstruction) structure for a five-level decomposition of the test ECG signal.

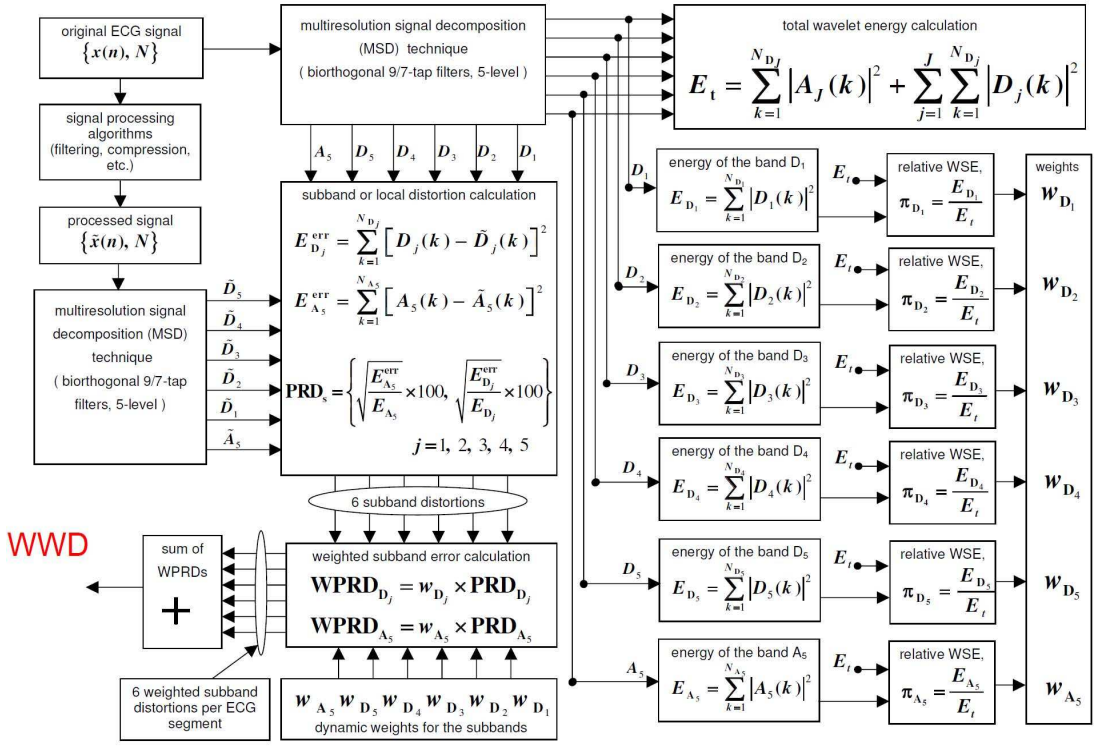

Figure 9: Block diagram of weighted wavelet distance (WWD) measure.

and the j^{th} level detail subband, respectively. Then, the dynamic weights that capture the actual contribution of the subbands are estimated as

$$w = \left[\frac{E_{\mathbf{A}_J}}{E_t}, \frac{E_{\mathbf{D}_J}}{E_t}, \frac{E_{\mathbf{D}_{J-1}}}{E_t}, , ... , \frac{E_{\mathbf{D}_1}}{E_t}\right]^T \tag{4}$$

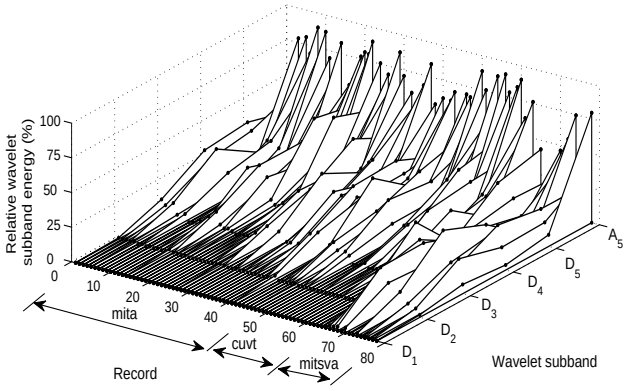

Figure 7: Relative wavelet subband energy (RWSE) distribution of each record taken from `mita`, `cuvt` and `mitsva` databases. We can note that the RWSE of the bands D_2 and D_1 is lesser as compared to the other bands.

Then, the weighted wavelet distance (WWD) is defined as [16]

$$\begin{aligned} \text{WWD} &= w_J \times \sqrt{\frac{\sum_{k=1}^{K_J} (\mathrm{A}_J[k] - \tilde{\mathrm{A}}_J[k])^2}{\sum_{k=1}^{K_j} (\mathrm{A}_J[k])^2}} \times 100 \quad (5) \\ &+ \sum_{j=1}^{J} w_j \times \sqrt{\frac{\sum_{k=1}^{K_j} (\mathrm{D}_j[k] - \tilde{\mathrm{D}}_j[k])^2}{\sum_{k=1}^{K_J} (\mathrm{D}_J[k])^2}} \times 100 \end{aligned}$$

where j is the subband, w_j is the dynamic weight of the j subband, K_j denotes the number of wavelet coefficients in j^{th} subband and $\mathrm{D}_j(k)$ is the k^{th} wavelet coefficient in j^{th} subband. The dynamic weights, w_j are estimated from the RWSEs of the subbands. The WWD measures the weighted normalized root-mean-squared difference between the subband coefficients of a current ECG beat and the subband coefficients of a past ECG beat. The overall architecture of the proposed weighted wavelet distance (WWD) metric is shown in 5. The WWD metric provides subband or local error estimation criterion that will focus on diagnostic quality for compressed signals. As will be demonstrated, the measure is insensitive to noise suppression and more sensitive to PQRST complex features distortion. Under noisy environments, the WWD metric reflects signal distortion and provides more meaningful results than the conventional distance metrics.

In this experiment, the commonly used dataset-I records (`mita` 100, 101, 102, 103, 107, 111, 115, 117, 118 and 119) are processed at a PRD1 value of 6%. The weighted local errors of the WWD and WWPRD [17] are shown in Table 1 and the reconstructed or compressed signals are shown in Fig. 10. It is observed that important diagnostic features are distorted and the small and short local waves are missing in Figs. 10 (a), (d), (h), (i), (k) and (l). In Figs. 10(h), (i) and (k), the duration of the small P wave is prolonged. Regardless of an apparent large error as reflected in the PRD's and in the WWPRD's, close examination of the signals of Fig. 10 reveals that all the local waves of the ECG and their diagnostic features are retained. The PRD1 and WWPRD have poor correlations with the visual quality of the two signals obtained for the widely used `mita` noisy records. In WWPRD criterion, insignificant errors in subbands D_2 and D_1 dominate the global error while significant errors in other bands may not reflect any contribution to the global error. This may lead to overlapping of the quality groups and to confusion in the judgement of the quality. The WWPRD criterion is not a subjectively meaningful measure since small and large numerical distortions do not correspond to "good" and "bad" subjective quality, respectively. Thus, the selection of upper bound distortion level is very difficult which is useful for clinical applications. The proposed WWD measure is superior over other measures in the sense that it is subjectively meaningful since the small and large values correspond to good and bad subjective quality, respectively. Thus, the WWD measure is much more suitable for evaluating compressed signals than the other measures, and naturally leads to a new method for quality control in ECG signal compression.

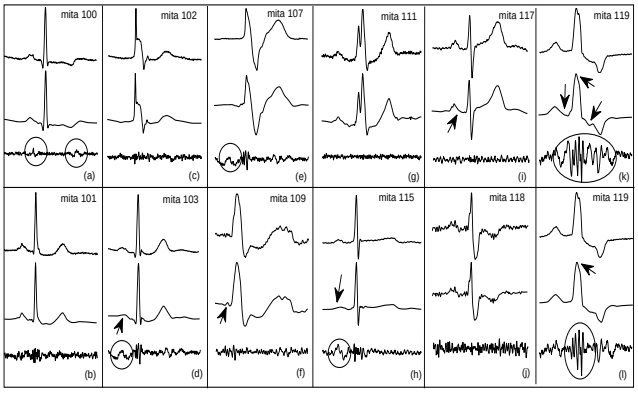

Figure 10: Compression results (PRD1=6%) of arrhythmia ECG signals extracted from dataset-I. Some of the distortion of the diagnostic features are marked in the compressed signals. From top to bottom, the plots display the original signal, the compressed signal and the difference between original and compressed signals.

4. RESULTS AND DISCUSSION

In this section, we evaluate the performance of the proposed algorithm using the well-known MIT-BIH arrhythmia database. It contains 48 half-hour of two-channel ECG recordings sampled at 360 Hz with 11-bit resolution over a 10 mV range. The ECG records from this database include signals with acceptable quality, sharp and tall P and T waves, negative QRS complex, small QRS complex, wider QRS complex, muscle noise, baseline drift, sudden changes in QRS amplitudes, sudden changes in QRS morphology, multiform premature ventricular contractions, long pauses and irregular heart rhythms.

In this work, we use three ECG features which include the heart rates, amplitudes of QRS complexes, shape of the PQRST morphology. The the shape and amplitude of PQRST complex morphology is the base for ECG diagnosis of various heart diseases. We use weighted wavelet distance metric for finding the similarity between shapes of the past PQRST and the present PQRST complexes. We apply a set of

Table 1: Performance evaluation of objective quality measures. Here, PRD1=6%

Rec.	Fig.	WWD:Weighted PRD (%) of bands							WWPRD:Weighted PRD (%) of bands						
	no.	A_5	D_5	D_4	D_3	D_2	D_1	Total	A_5	D_5	D_4	D_3	D_2	D_1	Total
100	10(a)	1.02	1.50	1.47	1.28	0.31	0.06	5.65	0.94	0.98	1.22	1.49	4.36	5.03	14.01
101	10(b)	1.56	1.11	1.51	1.06	0.67	0.08	5.99	1.52	1.01	0.74	1.42	5.49	5.33	15.52
102	10(c)	1.70	1.20	0.94	1.01	0.60	0.15	5.61	1.47	0.78	0.67	1.86	3.75	4.28	12.81
103	10(d)	2.25	2.77	1.40	0.33	0.18	0.02	6.97	4.54	1.31	1.14	2.93	3.00	3.63	16.56
107	10(e)	1.59	1.80	0.31	0.49	0.17	0.01	4.38	1.17	2.41	1.10	3.57	4.05	1.94	14.22
109	10(f)	3.89	0.50	0.58	0.29	0.22	0.05	5.52	3.07	0.31	1.61	3.79	6.51	4.43	19.73
111	10(g)	1.91	1.27	0.68	0.40	0.44	0.10	4.81	1.52	0.78	0.77	3.04	9.11	6.17	21.40
115	10(h)	1.22	1.49	1.91	0.94	0.27	0.03	5.86	2.19	1.18	0.82	2.22	2.15	3.53	12.09
117	10(i)	2.05	0.26	0.94	0.65	0.10	0.03	4.03	1.68	0.45	0.56	2.85	2.63	3.46	11.63
118	10(j)	2.18	1.16	0.55	1.10	0.48	0.03	5.50	1.98	0.44	1.43	3.02	8.46	3.65	18.96
119	10(k)	3.35	0.95	0.40	0.14	0.03	0.00	4.87	2.54	2.23	2.59	4.68	2.28	2.06	16.39
119	10(l)	3.35	0.51	0.27	0.14	0.03	0.00	4.30	2.55	1.21	1.72	4.68	2.28	2.06	14.50

Table 2: Performance of the proposed cardiac event change detection

Test Record	(P_{csb})	(P_f)
101	100	0
102	100	0
103	100	0
104	97.26	2.74
105	98.8	1.2
106	100	0
107	100	0
108	100	0
109	100	0
111	100	1.45
112	100	0
113	100	0
114	100	0
115	100	0
116	100	0
117	100	0
Average	99.76	0.317

bounds to decide whether two ECG beats may belong to the same class or not. The bounds for dissimilar ECG beats are:

- The RR-interval for the current ECG beat is less than 75% of the RR-interval for the past ECG beats.
- The amplitude ratio for the current ECG beat is less than 75% of the amplitude ratio for the past ECG beats.
- The value of weighted wavelet distance is greater than 5%.

The performance of the algorithm is validated by comparing the results of automatic annotations against groundtruth annotations. Each ECG record is divided into non-overlapping segments of 10 second duration. The average processing time required for performing our method on each 1-min ECG data in the MIT-BIH database is approximately 2.24 s. Each ECG segment is processed and the detected cardiac event change regions are verified by visual inspection. The following metrics are defined to evaluate the performance of the proposed algorithm.

- Probability of correctly detecting similar and dissimilar beats (P_{csb}): It is defined as the ratio of the total number of correctly detected similar and dissimilar beats to the total number of manually marked similar and dissimilar beats.
- Probability of falsely detecting beats (P_f): It is defined as total number of incorrectly detected similar and dissimilar beats to the total number of beats in the database.

Table 2 shows the overall accuracies obtained for all records from the well-known MIT-BIH arrhythmia database. We can observe that the performance of the proposed cardiac event change detection approach on the testing ECG records is comparable with the results in the ground truth report. The graphical user interface is shown in Figs. 11 and 12 for the test records 103 and 104.

5. CONCLUSION

In this paper, a novel automated ECG beat change detection approach is proposed and tested using the standard MIT-BIH arrhythmia database. The proposed approach consists of ECG beat extraction and weighted wavelet distance measure. Experiments show that the proposed approach achieves a better detection performance under signal with noise. In future work, we consider many clinical features for representation of ECG beat.

6. REFERENCES

[1] D. B. Geselowitz, "Origin of the electrocardiogram," *IEEE Engineering in Medicine and Biology Magazine*, vol. 13, no. 4, pp. 479-486, August/September 1994.

[2] A. Mattu, W. Brady, "ECGs for the emergency physician," 2003, BMJ Publishing Group, London.

[3] Report of committee on electrocardiography, American heart association, "Recommendations for standardization of leads and of specifications for instruments in electrocardiography and

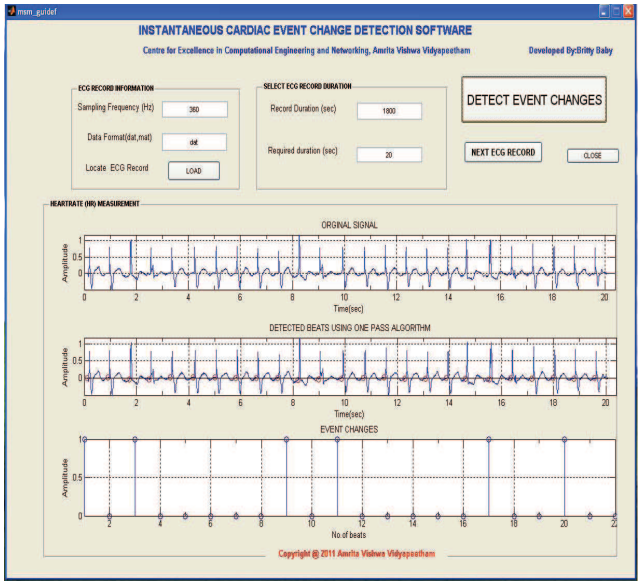

Figure 11: Outputs of the Cardiac Event Change Detector for the record 103.

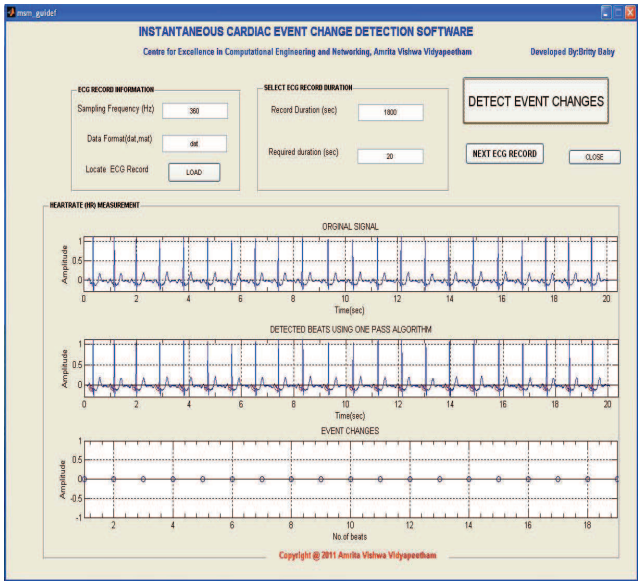

Figure 12: Outputs of the Cardiac Event Change Detector for the record 104.

vectorcardiography," *Circulation*, vol. XXXV, pp. 583-602, March 1967.

[4] Kligfield P, Gettes LS, Bailey J. J. Recommendations for the standardization and interpretation of the electrocardiogram: part I. The electrocardiogram and its technology: a scientific statement from the American Heart Association Electrocardiography and Arrhythmias Committee, Council on Clinical Cardiology; the American College of Cardiology Foundation; and the Heart Rhythm Society endorsed by the International Society for Computerized Electrocardiology. *Heart Rhythm*, vol. 4, no 3, 2007.

[5] N. P. Hughes, "Probabilistic models for automated ECG interval analysis," PhD thesis, University of Oxford, 2006.

[6] Lt'aszlt'o Gerencsr, Gyrgy Kozmann, Zsuzsanna Vt'agt'o, Kristt'of Haraszti, "The use of the SPSA method in ECG analysis," IEEE Trans. Biomedical Engineering, vol. 49, no. 10, pp. 1094-1101, 2002.

[7] N. V. Thakor, J. G. Webstor, W. J. Tompkins, "Estimation of QRS complex power spectra for design of a QRS filter," *IEEE Trans. Biomedical Engineering*, vol. BME-31, no. 11, pp. 702-705, 1984.

[8] G. J. Guang, W. J. Tompkins, "High-frequency electrocardiogram analyzer," *IEEE Trans. Biomedical Engineering*, vol. BME-33, no. 12, pp. 1137-1140, 1986.

[9] László Gerencsér, György Kozmann, Zsuzsanna Vágó, Kristóf Haraszti, "The Use of the SPSA Method in ECG Analysis," *IEEE Trans. Biomedical Engineering*, vol. 49, no. 10, pp. 1094-1101, 2002.

[10] L. Cuiwei, C. Zheng, C. Tai, "Detection of ECG characteristic points using wavelet transforms," *IEEE Trans. Biomedical Engineering,* vol. 42, no. 1, pp. 21-28, 1995.

[11] K. Park, B. Cho, D. Lee, S. Song, J. Lee, Y. Chee, I. Kim and S. Kim, "Hierarchical support vector machine based heart beat classification using higher order statistics and hermite basis function." *Computers in Cardiology,* pp. 229-232, 2008.

[12] P. de Chazal, M. OŠDwyer and R. B. Reilly, "Automatic Classification of Heart beats using ECG Morphology and Heart beat Interval Features," *IEEE Trans. on Biomedical Engineering,* vol. 51, no. 7, pp. 1196-1206, 2004.

[13] H. H. Haseena, A. T. Mathew, J. K. Paul, "Fuzzy clustered probabilistic and multi layered feed forward neural networks for electrocardiogram arrhythmia classification," *Journal of Medical Systems,* pp. 1-10, 2009.

[14] M. G. Tsipouras, D. I. Fotiadis, D. Sideris, "An arrhythmia classification system based on the RR-interval signal," *Artificial Intelligence in Medicine,* vol. 33, pp. 237-250, 2005.

[15] P. Kathirvel, M. Sabarimalai Manikandan, S. R. M. Prasanna, K. P. Soman, "An efficient R-peak detection based on new nonlinear transformation and first-order Gaussian differentiator" *Cardiovascular Engineering and Technology, Spinger*, DOI: 10.1007/s13239-011-0065-3, 2011.

[16] M. Sabarimalai Manikandan, S. Dandapat, "Wavelet energy based diagnostic distortion measure for ECG", *Biomed. Signal Process. and Control.,* vol. 2, no. 2, pp. 80-96, 2007.

[17] A. S. Al-Fahoum, "Quality assessment of ECG compression techniques using a wavelet-based diagnostic measure," *IEEE Trans. Information Technology in Biomedicine,* vol. 10, no. 1, pp. 182-191, 2006.